Numerical study for mixed convection flow of Oldroyd-B nanofluid subject to activation energy and binary chemical reaction

Dina ABUZAID[1] and Malik Zaka ULLAH[1*]

[1] Department of Mathematics, Faculty of Science, King Abdulaziz University, Jeddah 21589, Saudi Arabia

[*] Corresponding author E-mail: zmalek@kau.edu.sa (Malik Zaka ULLAH)

Abstract: This attempt discusses mixed convection Oldroyd-B nanoliquid flow over a doubly stratified surface in existence of activation energy. Impacts of Brownian diffusion and thermophoretic are additionally accounted. The non-linear frameworks are simplified by suitable variables. Shooting method is utilized to develop numeric solution of resulting issue. Graphs have been composed just to explore that how concentration and the temperature are impacted by different developing flow factors. Mass and heat transport rates are additionally tabulated and dissected. Furthermore, the temperature and concentration distributions are enhanced for larger thermophoresis parameter.

Keywords: Mixed convection flow; Double stratification; Oldroyd-B fluid; Binary chemical reaction; Nanoparticles; Arrhenius activation energy.

1. Introduction

The nanoparticle of size under 100 nm deferred into a standard fluid is named as nanoliquid. The essentialness of nanofluid is expected to their distinctive thermophysical qualities. Nanofluids show enormous capacity to lead power and heat, so it has a critical impact in industry. Nanoliquids have gotten extraordinary enthusiasm for its wide applications, for example, electronic chip cooling, hybrid powered machines, progressed atomic frameworks, laser-helped sedate conveyance, solar liquid heating, microchips, excessively proficient magnets and optoelectronics and so on. Just because, Choi [1] exhibited the term nanoparticle inundated into a common fluid. Buongiorno [2] presented a numerical model for warm transport in nanoliquid, including the impacts of Brownian scattering and thermophoretic dispersion. Further applicable examinations on nanofluids are cited by the investigations [3-18].

Species of concentration contrast exist in a blend subject to mass transport wonder. By fluctuating centralization of species in blend move those from high focus locale to low fixation area. Least mandatory vitality that is needed by reactants before occuring substance reaction is termed as activation energy. Mass move mechanism with concoction reaction with activation energy by and the large discovers practicals in mechanics of oil and water emulsions, synthetic building, nourishment preparing etc. Right off bat common convection flow of paired blend in porous space subject to initiation vitality is proposed by Bestman [19]. Makinde et al. [20] numerically examined insecure normal convective stream with enactment vitality and nth-request response. Maleque [21] discussed endothermic/exothermic response in mixed convective streams with initiation vitality. Changed Arrhenius work has been utilized by Awad et al. [22] so as to consider flimsy pivoting stream of parallel liquid past a rash twisted surface. Casson liquid stream subject to initiation vitality is tended to by Abbas et al. [23]. Shafique et al. [24] inspected numerically the

pivoting viscoelastic stream fusing artificially receptive species with actuation vitality. Anuradha and Yegammai [25] talked about paired concoction response and initiation vitality in radiative hydromagnetic nanoliquid flow by vertical surface. Khan et al. [26] analyzed impacts of enactment vitality and entropy in radiative nanomaterial flow. Further ongoing endeavors on activation energy are cited by attempts [27-30].

Inspired by above mentioned attempts, the motivation here is to explore importance of binary chemical response and activation energy in mixed convection Oldroyd-B nanoliquid flow with solutal and thermal stratifications. Random movement and thermophoretic phenomenas occur in the existence of nanofluid. Resulting scientific framework is understood numerically via shooting technique. Concentration, temperature, Sherwood and Nusselt factors are also analyzed.

2. Problem development

We examine 2D doubly stratified mixed convection Oldroyd-B nanoliquid flow with binary chemical response and activation energy. Flow is induced by extending sheet at $y = 0$. Flow occupies the region $y > 0$ (see Fig. 1). Brownian dispersion and thermophoretic impacts are likewise present. The governing expressions of Oldroyd-B nanoliquid flow are [28, 31]:

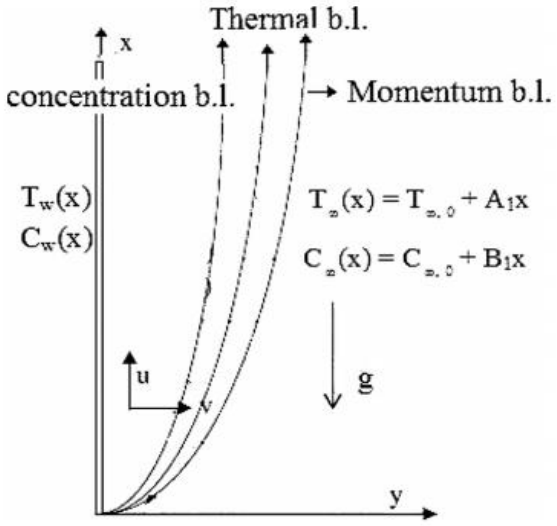

Fig. 1: Flow model and coordinate system.

$$\frac{\partial u}{\partial x} + \frac{\partial v}{\partial y} = 0, \tag{1}$$

$$u\frac{\partial u}{\partial x} + v\frac{\partial u}{\partial y} + \lambda_1\left(\begin{array}{c} u^2\frac{\partial^2 u}{\partial x^2} + v^2\frac{\partial^2 u}{\partial y^2} \\ + 2uv\frac{\partial^2 u}{\partial x \partial y} \end{array}\right) = \nu\frac{\partial^2 u}{\partial y^2} + \nu\lambda_2\left(\begin{array}{c} u\frac{\partial^3 u}{\partial x \partial y^2} + v\frac{\partial^3 u}{\partial y^3} \\ -\frac{\partial u}{\partial x}\frac{\partial^2 u}{\partial y^2} - \frac{\partial u}{\partial y}\frac{\partial^2 v}{\partial y^2} \end{array}\right)$$
$$+ g\left(\beta_T\left(T - T_\infty\right) + \beta_C\left(C - C_\infty\right)\right), \tag{2}$$

$$u\frac{\partial T}{\partial x} + v\frac{\partial T}{\partial y} = \alpha\frac{\partial^2 T}{\partial y^2} + \frac{(\rho c)_p}{(\rho c)_f}\left(D_B\left(\frac{\partial T}{\partial y}\frac{\partial C}{\partial y}\right) + \frac{D_T}{T_\infty}\left(\frac{\partial T}{\partial y}\right)^2\right), \tag{3}$$

$$u\frac{\partial C}{\partial x}+v\frac{\partial C}{\partial y}=D_B\frac{\partial^2 C}{\partial y^2}+\frac{D_T}{T_\infty}\left(\frac{\partial^2 T}{\partial y^2}\right)-k_r^2\left(C-C_\infty\right)\left(\frac{T}{T_\infty}\right)^n\exp\left(-\frac{E_a}{\kappa T}\right). \tag{4}$$

Subjected boundary conditions are [31]:

$$u=U_w(x),\ v=0,\ T=T_w(x),\ C=C_w(x)\ \text{at}\ y=0, \tag{5}$$

$$u\to 0, T\to T_\infty(x)=T_{\infty,0}+A_1x,\ C\to C_\infty(x)=C_{\infty,0}+B_1x\ \text{as}\ y\to\infty, \tag{6}$$

in which u and v stand for velocities in $x-$ and $y-$axes, n for fitted rate constant, E_a for activation energy, μ for dynamic viscosity, $(\rho c)_f$ for heat capacity of fluid, D_B for Brownian factor, κ for Boltzmann constant, T for temperature, λ_1 for relaxation time, $\nu=\mu/\rho$ for kinematic viscosity, β_C for concentration expansion factor, $(\rho c)_p$ for effective heat capacity of nanoparticles, k_r for reaction rate, k for thermal conductivity, λ_2 for retardation time, g for gravitational acceleration, D_T for thermophoretic factor, β_T for thermal expansion factor, ρ for density, C for concentration, $\alpha=k/(\rho c)_f$ for thermal diffusivity, T_∞ and T_w for ambient and surface temperatures and C_∞ and C_w for ambient and surface concentrations. Thus

$$U_w(x)=cx,\ T_w(x)=T_{\infty,0}+M_1x,\ C_w(x)=C_{\infty,0}+N_1x, \tag{7}$$

where c, A_1, B_1, M_1, N_1, $T_{\infty,0}$ and $C_{\infty,0}$ stand for positive constants. Non-dimensional variables are defined by

$$\left.\begin{aligned} u=cxf'(\eta),\ v=-\sqrt{c\nu}\,f(\eta),\ \eta=\sqrt{\tfrac{c}{\nu}}y,\\ \theta(\eta)=\tfrac{T-T_{\infty,0}}{\Delta T}-\tfrac{A_1x}{\Delta T},\ \Delta T=T_w(x)-T_{\infty,0}=M_1x,\\ \phi(\eta)=\tfrac{C-C_{\infty,0}}{\Delta C}-\tfrac{B_1x}{\Delta C},\ \Delta C=C_w(x)-C_{\infty,0}=N_1x. \end{aligned}\right\} \tag{8}$$

Equation (1) is now identically verified and Eqs. $(2)-(7)$ yield

$$f'''+ff''-f'^2+\beta_1\left(2ff'f''-f^2f'''\right)+\beta_2\left(f'^2-ff^{iv}\right)+\lambda(\theta+N\phi)=0, \tag{9}$$

$$\theta''+\Pr\left(f\theta'-f'\theta-\varepsilon_1f'+N_b\theta'\phi'+N_t\theta'^2\right)=0, \tag{10}$$

$$\phi''+Sc\left(f\phi'-f'\phi-\varepsilon_2f'\right)+\frac{N_t}{N_b}\theta''-\sigma Sc(1+\delta\theta)^n\phi\exp\left(-\frac{E}{1+\delta\theta}\right)=0, \tag{11}$$

$$f=0,\ f'=1,\ \theta=1-\varepsilon_1,\ \phi=1-\varepsilon_2\ \text{at}\ \eta=0, \tag{12}$$

$$f'\to 0,\ f''\to 0,\ \theta\to 0,\ \varphi\to 0\ \text{as}\ \eta\to\infty. \tag{13}$$

In above expressions N_b stands for Brownian motion parameter, β_2 and β_1 for Deborah numbers in terms of retardation and relaxation times, ε_2 for solutal stratification, Re_x for local Reynolds number, δ for temperature difference parameter, λ for mixed convection number, N_t for thermophoresis number, Gr_x for Grashof parameter, E for nondimensional activation energy, σ for chemical reaction parameter, N for buoyancy ratio, $\Pr$ for Prandtl number, ε_1 for thermal stratification and Sc for Schmidt number. These parameters are expressed as follows:

$$\left.\begin{array}{c}\beta_1=\lambda_1 c,\ \beta_2=\lambda_2 c,\ \lambda=\frac{Gr_x}{\mathrm{Re}_x^2},\ Gr_x=\frac{g\beta_T\Delta T x^3}{\nu^2},\ \delta=\frac{T_w-T_\infty}{T_\infty},\\ \mathrm{Re}_x=\frac{U_w x}{\nu},\ N=\frac{\beta_C\Delta C}{\beta_T\Delta T},\ \mathrm{Pr}=\frac{\nu}{\alpha},\ N_b=\frac{(\rho c)_p}{(\rho c)_f}\frac{D_B\Delta C}{\nu},\ N_t=\frac{(\rho c)_p}{(\rho c)_f}\frac{D_T\Delta T}{\nu T_\infty},\\ E=\frac{E_a}{\kappa T_\infty},\ \varepsilon_1=\frac{x}{\Delta T}\frac{d}{dx}\left[T_\infty(x)\right],\ Sc=\frac{\nu}{D_B},\ \varepsilon_2=\frac{x}{\Delta C}\frac{d}{dx}\left[C_\infty(x)\right],\ \sigma=\frac{k_r^2}{c}.\end{array}\right\} \quad (14)$$

Local Nusselt Nu_x and the Sherwood Sh_x factors are stated by

$$Nu_x=-\frac{x}{(T_w-T_\infty)}\frac{\partial T}{\partial y}\bigg|_{y=0}=-(\mathrm{Re}_x)^{1/2}\theta'(0), \quad (15)$$

$$Sh_x=-\frac{x}{(C_w-C_\infty)}\frac{\partial C}{\partial y}\bigg|_{y=0}=-(\mathrm{Re}_x)^{1/2}\phi'(0). \quad (16)$$

3. Graphical results and discussion

The arrangements of administering framework are figured by utilizing shooting strategy. This segment presents impacts of various pertinent parameters including Deborah numbers β_2 and β_1, mixed convection parameter λ, thermophoresis parameter N_t, activation energy E, Brownian movement parameter N_b, warm stratification parameter ε_1, concoction response parameter σ and solutal stratification ε_2 on temperature $\theta(\eta)$ and concentration $\phi(\eta)$. Variation in temperature $\theta(\eta)$ for varying Deborah number β_1 is appeared in Fig. 2. Here temperature profile is more for bigger Deborah number β_1. Impact of Deborah number β_2 on temperature $\theta(\eta)$ is shown in Fig. 3. It is plainly indicated that temperature $\theta(\eta)$ is diminishing capacity of Deborah number β_2. A correlation of Figs. 2 and 3 shows that β_1 and β_2 have very inverse consequences for temperature field. Physically β_1 includes unwinding time while β_2 comprises of hindrance time. Bigger unwinding time prompts higher temperature while bigger hindrance time compares to a lower temperature. In this way an improvement in β_1 produces more temperature while bigger β_2 portrays less temperature. Fig. 4 presents bigger estimations of blended convection parameter λ comparing to bring down temperature $\theta(\eta)$. Fig. 5 presents impact of warm stratification ε_1 on temperature $\theta(\eta)$. Temperature $\theta(\eta)$ is diminishing capacity of the warm stratification parameter ε_1. Physically nearness of warm stratification impact diminishes viable temperature contrast among surface and encompassing liquid which prompts a flimsier temperature. It is additionally seen that instance of recommended surface temperature is recouped when $\varepsilon_1=0$. Thermophoresis and Brownian movement impacts on temperature $\theta(\eta)$ are exhibited in Figs. 6 and 7 individually. Temperature profile is higher for bigger estimations of thermophoresis and Brownian movement. Physically nearness of nanoparticles builds warm conductivity of liquid. An expansion in thermophoresis and Brownian movement compares to high warm conductivity. Such high warm conductivity makes upgrade in the temperature field. Fig. 8 shows variety in concentration $\phi(\eta)$ for different estimations of

Deborah number β_1 . Here concentration is improved with expansion in the Deborah number β_1 . Fig. 9 displays that bigger Deborah number β_2 produces a decrease in concentration $\phi(\eta)$. Fig. 10 shows change in concentration $\phi(\eta)$ comparing to various estimations of blended convection parameter λ. Clearly concentration $\phi(\eta)$ is lower for bigger estimations of blended convection parameter λ. Impact of solutal stratification ε_2 on concentration $\phi(\eta)$ is plotted in Fig. 11. It is unmistakably noted that concentration $\phi(\eta)$ is reduced when solutal stratification ε_2 enlarges. For $\varepsilon_2 = 0$, recommended surface concentration circumstance is accomplished. Impact of thermophoresis parameter N_t on concentration $\phi(\eta)$ is shown in Fig. 12. Concentration $\phi(\eta)$ is expanding capacity of thermophoresis parameter N_t. Fig. 13 shows that concentration $\phi(\eta)$ is lower for bigger estimations of Brownian movement parameter N_b. Fig. 14 delineates that bigger estimations of compound response parameter σ prompts lower concentration. Fig. 15 clarifies effect of E on concentration $\phi(\eta)$. An improvement in E prompts higher concentration $\phi(\eta)$. Table 1 presents numerical estimations of heat move rate $-\theta'(0)$ for particular estimations of blended convection parameter λ. It is seen that heat move rate is higher when expanding estimations of blended convection parameter λ are accounted. Table 2 delineates mass move rate $-\phi'(0)$ for particular values of blended convection parameter λ. Here we saw that mass move rate has higher estimations for bigger blended convection parameter λ.

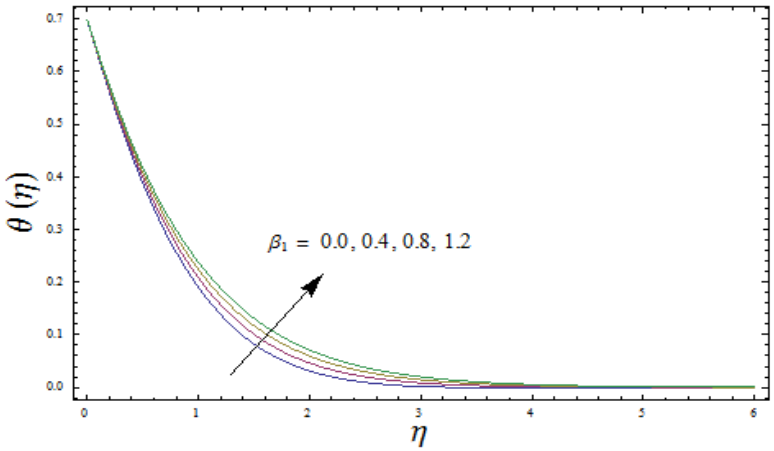

Fig. 2: Curves of $\theta(\eta)$ for β_1.

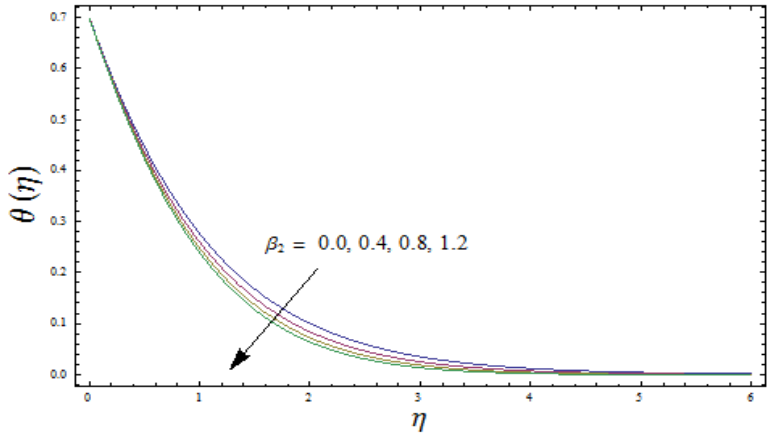

Fig. 3: Curves of $\theta(\eta)$ for β_2.

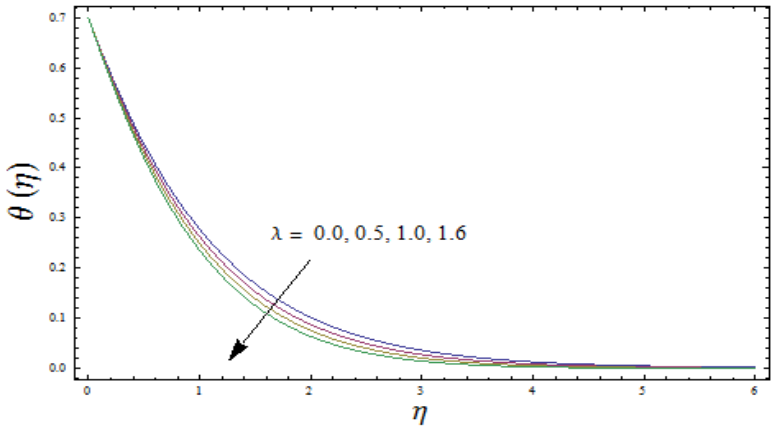

Fig. 4: Curves of $\theta(\eta)$ for λ.

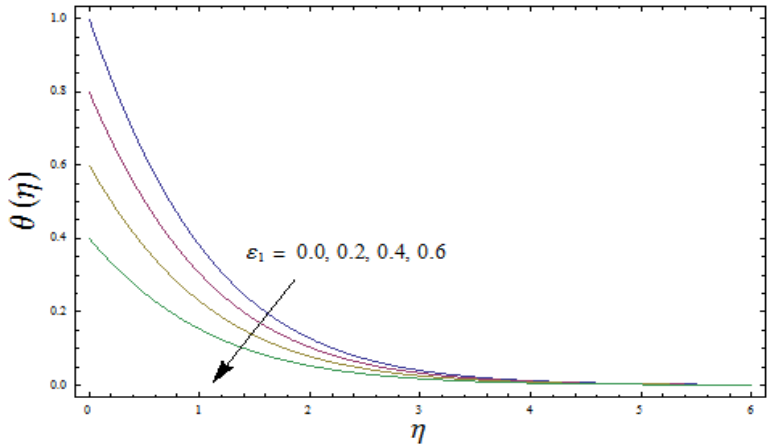

Fig. 5: Curves of $\theta(\eta)$ for ε_1.

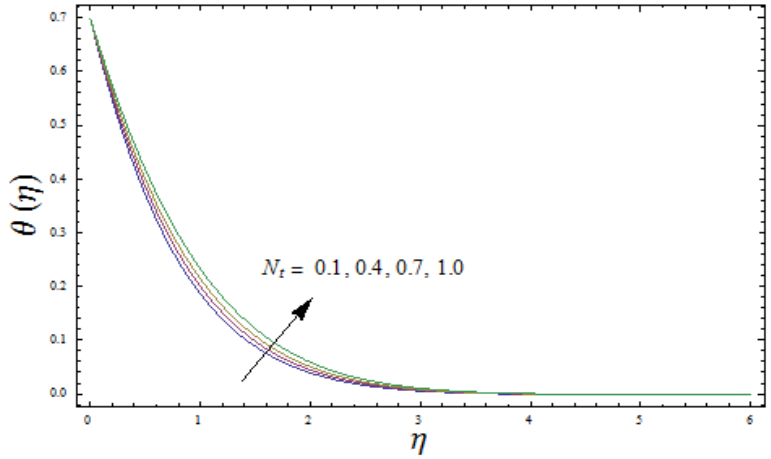

Fig. 6: Curves of $\theta(\eta)$ for N_t.

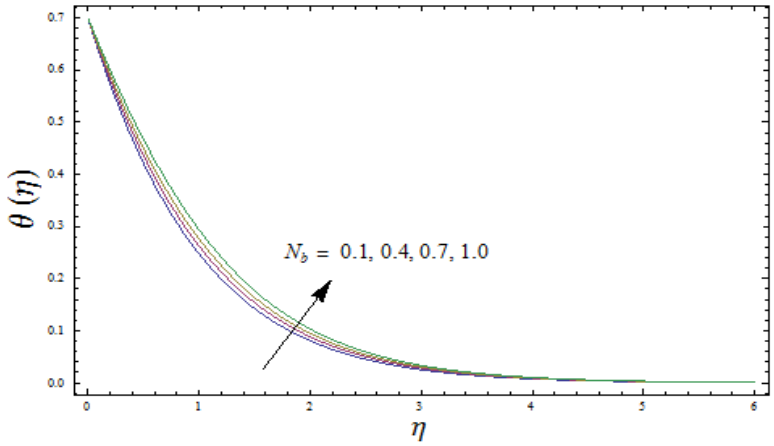

Fig. 7: Curves of $\theta(\eta)$ for N_b.

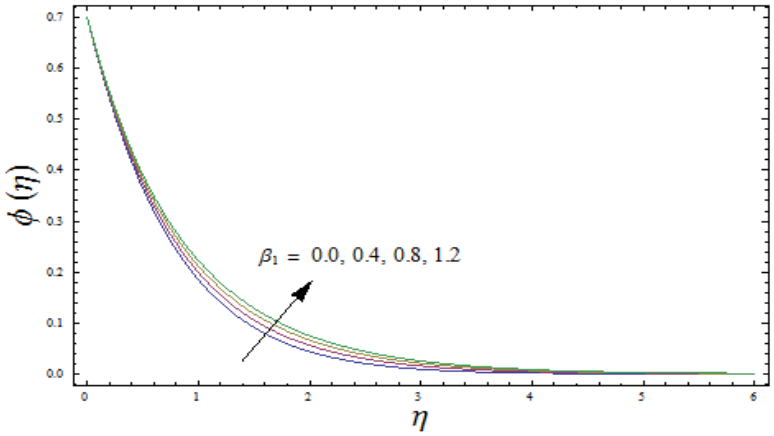

Fig. 8: Curves of $\phi(\eta)$ for β_1.

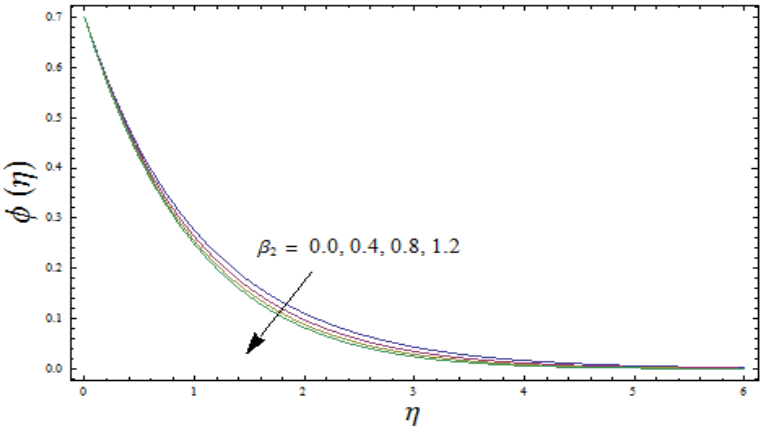

Fig. 9: Curves of $\phi(\eta)$ for β_2.

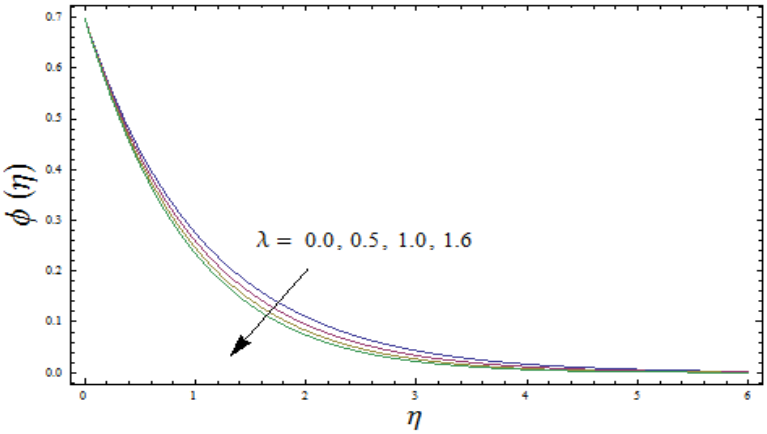

Fig. 10: Curves of $\phi(\eta)$ for λ.

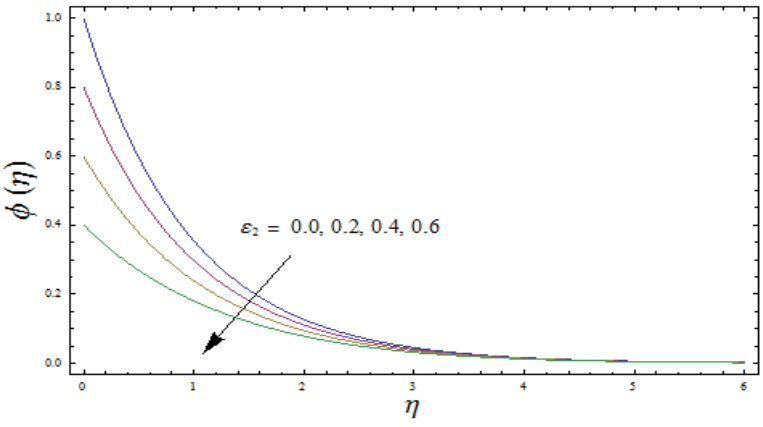

Fig. 11: Curves of $\phi(\eta)$ for ε_2.

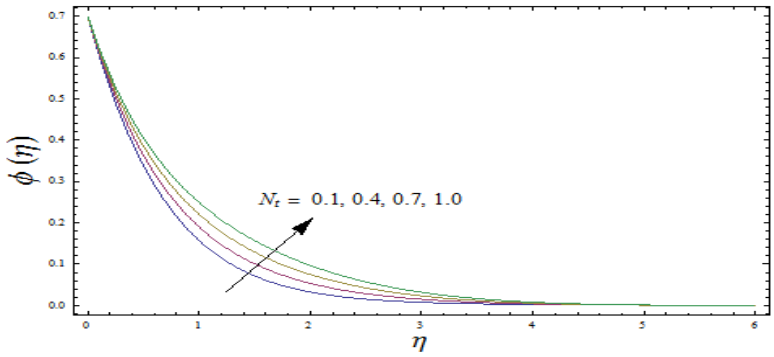

Fig. 12: Curves of $\phi(\eta)$ for N_t.

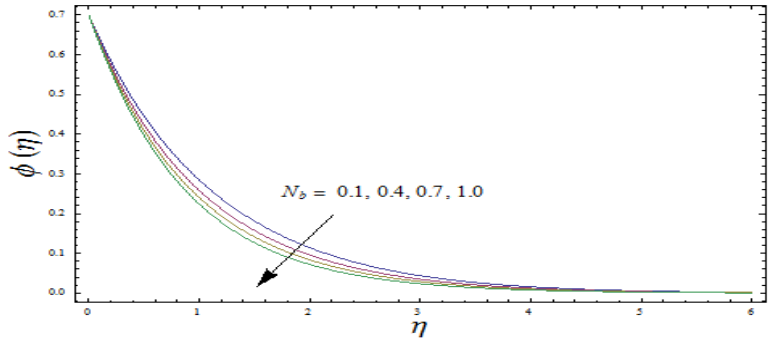

Fig. 13: Curves of $\phi(\eta)$ for N_b.

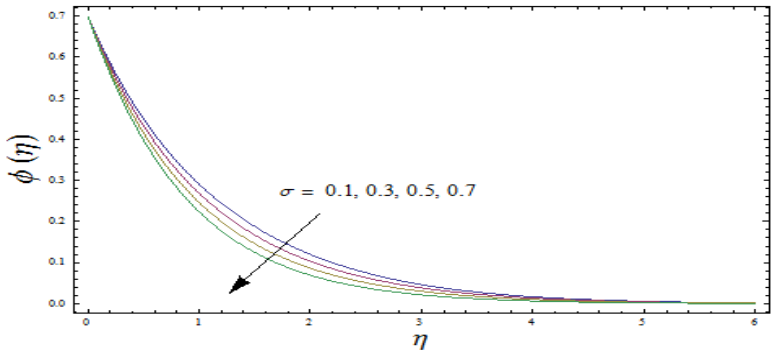

Fig. 14: Curves of $\phi(\eta)$ for σ.

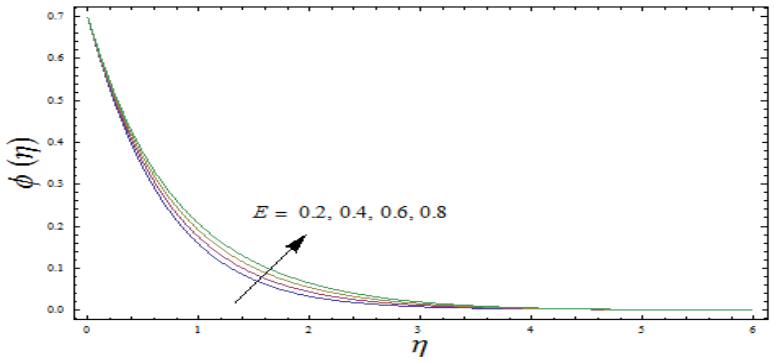

Fig. 15: Curves of $\phi(\eta)$ for E.

Table 1: Heat transfer rate $-\theta'(0)$ for varying λ when $\beta_1 = \beta_2 = 0.2$, $N = 0.1$, $\delta = 0.3$, $E = 0.5$, $N_t = 0.2$, $\Pr = Sc = 1.0$, $N_b = 0.5$ and $\varepsilon_1 = \varepsilon_2 = 0.3$.

λ	0.0	0.2	0.4	0.6
$-\theta'(0)$	0.60305	0.61415	0.62231	0.62975

Table 2: Mass transfer rate $-\phi'(0)$ for varying λ when $\beta_1 = \beta_2 = 0.2$, $N = 0.1$, $\delta = 0.3$, $E = 0.5$, $N_t = 0.2$, $\Pr = Sc = 1.0$, $N_b = 0.5$ and $\varepsilon_1 = \varepsilon_2 = 0.3$.

λ	0.0	0.2	0.4	0.6
$-\phi'(0)$	0.66692	0.67715	0.68496	0.69205

4. Conclusions

Importance of double stratification in mixed convection Oldroyd-B nanoliquid flow with binary chemical response and activation energy is inspected. Both temperature and concentration are enhanced when we increment β_1. Both temperature and concentration have been reduced for larger estimations of mixed convective number. Impacts of solutal and thermal stratification numbers on concentration and temperature respectively are similar. The present results reduces to Newtonian fluid flow situation when $\beta_1 = \beta_2 = 0$.

Acknowledgment: This project was funded by the Deanship of Scientific Research (DSR) at King Abdulaziz University, Jeddah, under grant no. G: 1458-247-1440. The authors, therefore, acknowledge with thanks DSR for technical and financial support.

References

[1] S.U.S. Choi, Enhancing thermal conductivity of fluids with nanoparticles, USA, ASME, FED 231/MD, 66 (1995) 99-105.

[2] J. Buongiorno, Convective transport in nanofluids, J. Heat Transfer, 128 (2006) 240-250.

[3] J.A. Eastman, S.U.S. Choi, S. Li, W. Yu and L.J. Thompson, Anomalously increased effective thermal conductivities of ethylene glycol-based nanofluids containing copper nanoparticles, Appl. Phys. Lett. 78 (2001) 718-720.

[4] R.K. Tiwari and M.K. Das, Heat transfer augmentation in a two-sided lid-driven differentially heated square cavity utilizing nanofluid, Int. J. Heat Mass Transf., 50 (2007) 2002-2018.

[5] E. Abu-Nada and H.F. Oztop, Effects of inclination angle on natural convection in enclosures filled with Cu-water nanofluid, Int. J. Heat Fluid Flow, 30 (2009) 669-678.

[6] J.A. Khan, M. Mustafa, T. Hayat, M.A. Farooq, A. Alsaedi and S.J. Liao, On model for three-dimensional flow of nanofluid: An application to solar energy, J. Mol. Liq., 194 (2014) 41-47.

[7] S. Mansur and A. Ishak, Three-dimensional flow and heat transfer of a nanofluid past a permeable stretching sheet with a convective boundary condition, AIP Conference Proceedings, 1614 (2014) 906.

[8] T. Hayat, T. Muhammad, A. Alsaedi and M.S. Alhuthali, Magnetohydrodynamic

three-dimensional flow of viscoelastic nanofluid in the presence of nonlinear thermal radiation, J. Magn. Magn. Mater., 385 (2015) 222-229.

[9] T. Muhammad, A. Alsaedi, S.A. Shehzad and T. Hayat, A revised model for Darcy-Forchheimer flow of Maxwell nanofluid subject to convective boundary condition, Chinese J. Phys., 55 (2017) 963-976.

[10] T. Hayat, T. Muhammad, S.A. Shehzad and A. Alsaedi, An analytical solution for magnetohydrodynamic Oldroyd-B nanofluid flow induced by a stretching sheet with heat generation/absorption, Int. J. Thermal Sci., 111 (2017) 274-288.

[11] T. Muhammad, A. Alsaedi, T. Hayat and S.A. Shehzad, A revised model for Darcy-Forchheimer three-dimensional flow of nanofluid subject to convective boundary condition, Results Phys., 7 (2017) 2791-2797.

[12] T. Hayat, T. Muhammad, S.A. Shehzad and A. Alsaedi, On magnetohydrodynamic flow of nanofluid due to a rotating disk with slip effect: A numerical study, Comp. Methods Appl. Mech. Eng., 315 (2017) 467-477.

[13] Z. Hussain, T. Hayat, A. Alsaedi and B. Ahmad, Three-dimensional convective flow of CNTs nanofluids with heat generation/absorption effect: A numerical study, Comp. Methods Appl. Mech. Eng., 329 (2018) 40-54.

[14] F. Selimefendigil and H.F. Oztop, Mixed convection of nanofluids in a three dimensional cavity with two adiabatic inner rotating cylinders, Int. J. Heat Mass Transfer, 117 (2018) 331-343.

[15] T. Muhammad, D.C. Lu, B. Mahanthesh, M.R. Eid, M. Ramzan and A. Dar, Significance of Darcy-Forchheimer porous medium in nanofluid through carbon nanotubes, Commun. Theoret. Phys., 70 (2018) 361.

[16] T. Hayat, M. Khan, T. Muhammad and A. Alsaedi, On model for three-dimensional flow of nanofluid with heat and mass flux boundary conditions, J. Thermal Sci. Eng. Appl., 10 (2018) 031003.

[17] B. Mahanthesh, B.J. Gireesha, I.L. Animasaun, T. Muhammad and N.S. Shashikumar, MHD flow of SWCNT and MWCNT nanoliquids past a rotating stretchable disk with thermal and exponential space dependent heat source, Physica Scripta, 94 (2019) 085214.

[18] R.S. Saif, T. Hayat, R. Ellahi, T. Muhammad and A. Alsaedi, Darcy-Forchheimer flow of nanofluid due to a curved stretching surface, Int. J. Numer. Methods Heat Fluid Flow, 29 (2019) 2-20.

[19] A.R. Bestman, Natural convection boundary layer with suction and mass transfer in a porous medium, Int. J. Energy Res., 14 (1990) 389-396.

[20] O.D. Makinde, P.O. Olanrewaju and W.M. Charles, Unsteady convection with chemical reaction and radiative heat transfer past a flat porous plate moving through a binary mixture, Africka Matematika 22 (2011) 65-78.

[21] K.A. Maleque, Effects of exothermic/endothermic chemical reactions with Arrhenius activation energy on MHD free convection and mass transfer flow in presence of

thermal radiation, J. Thermodyn., 2013 (2013) 692516.

[22] F.G. Awad, S. Motsa and M. Khumalo, Heat and mass transfer in unsteady rotating fluid flow with binary chemical reaction and activation energy, Plos One 9 (2014) e107622.

[23] Z. Abbas, M. Sheikh and S.S. Motsa, Numerical solution of binary chemical reaction on stagnation point flow of Casson fluid over a stretching/shrinking sheet with thermal radiation, Energy 95 (2016) 12-20.

[24] Z. Shafique, M. Mustafa and A. Mushtaq, Boundary layer flow of Maxwell fluid in rotating frame with binary chemical reaction and activation energy, Results Phys. 6 (2016) 627-633.

[25] S. Anuradha and M. Yegammai, MHD radiative boundary layer flow of nanofluid past a vertical plate with effects of binary chemical reaction and activation energy, Glob. J. Pure Appl. Math., 13 (2017) 6377-6392.

[26] M.I. Khan, S. Qayyum, T. Hayat, M. Waqas, M.I. Khan and A. Alsaedi, Entropy generation minimization and binary chemical reaction with Arrhenius activation energy in MHD radiative flow of nanomaterial, J. Mol. Liq., 259 (2018) 274-283.

[27] T. Hayat, A. Aziz, T. Muhammad and A. Alsaedi, Numerical simulation for Darcy-Forchheimer 3D rotating flow subject to binary chemical reaction and Arrhenius activation energy, J. Central South Uni., 26 (2019) 1250-1259.

[28] T. Hayat, A. Aziz, T. Muhammad and A. Alsaedi, Effects of binary chemical reaction and Arrhenius activation energy in Darcy-Forchheimer three-dimensional flow of nanofluid subject to rotating frame, J. Thermal Anal. Calorimet., 136 (2019) 1769-1779.

[29] M. Asma, W.A.M. Othman and T. Muhammad, Numerical study for Darcy-Forchheimer flow of nanofluid due to a rotating disk with binary chemical reaction and Arrhenius activation energy, Mathematics, 7 (2019) 921.

[30] M. Asma, W.A.M. Othman, T. Muhammad, F. Mallawi and B.R. Wong, Numerical study for magnetohydrodynamic flow of nanofluid due to a rotating disk with binary chemical reaction and Arrhenius activation energy, Symmetry, 11 (2019) 1282.

[31] T. Hayat, T. Muhammad, S.A. Shehzad and A. Alsaedi, Temperature and concentration stratification effects in mixed convection flow of an Oldroyd-B fluid with thermal radiation and chemical reaction, PloS One, 10 (2015) e0127646.

Submitted: 14.02.2020.
Revised: 05.04.2020.
Accepted: 09.04.2020.